Formation of the Three-Ring Structure Around Supernova 1987A

T. Tanaka[1]* and H. Washimi[2]

From a magnetohydrodynamic simulation, we reproduce a three-ring structure in the circumstellar space of the supernova (SN) 1987A observed by the Hubble Space Telescope. When a star develops from a red supergiant (RSG) to a blue supergiant (BSG) just before the SN explosion, a wind-wind interaction occurs between the slow stellar wind from the RSG and the subsequent fast stellar wind from the BSG. This process is simulated numerically under an assumption that the density and velocity distributions around the RSG are anisotropic owing to the existence of toroidal magnetic field and coronal holes. The three rings with observed size and position are reproduced by the magnetic pinch effect and amplification of initial density asymmetry through the dynamical interaction.

Recent observations by the Hubble Space Telescope (HST) show many ring-like structures of circumstellar nebulae that are associated with the death of stars, such as the three-ring structure around SN 1987A (Fig. 1). The equatorial ring (ER) of SN 1987A is on the equatorial plane of the star and has a radius of 0.7 light years (ly). The two outer rings (ORs), at latitudes of about 45° in both hemispheres, have radii about twice that of the ER (i.e., 1.4 ly). These three rings are the traces of high-density regions illuminated through the recombination process of atoms ionized by the ultraviolet flash of SN explosion. Here we clarify the formation process of the three-ring structure by computer simulations.

The colliding wind model (*1*) explains the ring structures of planetary nebulae on the basis of the hydrodynamic interaction between fast and slow stellar winds. When the progenitor of the SN is a RSG, a dense and slow RSG wind steadily expands from the star into the circumstellar space. Just before the SN explosion the RSG evolves into a BSG, and dilute and fast stellar wind from the BSG begins to expand outward into the preexisting RSG wind, sweeping up the matter of the RSG wind at the expanding front (*2*). When the RSG wind is spherically nonsymmetric, a ring structure is formed from the high-density RSG wind around the equator. In addition, the magnetohydrodynamic (MHD) effect makes the ring structure more distinct (*3*).

We assume that the star has a dipole magnetic field, and that the ionized stellar wind has anisotropic density and velocity distributions: The stellar wind is fast in the high-latitude coronal hole region and slow in the low-latitude region. These assumptions are introduced by analogy to recent solar wind observations by the inner-heliospheric polar-orbiting spacecraft Ulysses (*4*). The magnetic field is dragged out and wound up to the toroidal field in the circumstellar space by the radially expanding stellar wind and stellar rotation. To explain the three-ring structure, we treat the wind-wind interaction in a MHD regime with anisotropic RSG and BSG winds.

An important advantage of our simulation is that it adopts a highly accurate scheme for the MHD computation. We use the finite-volume total variation diminishing scheme with a third-order numerical flux based on the monotonic upstream scheme for the conservation law approach (*5*). Our assumptions are implemented in the MHD simulation by specifying the inner boundary conditions. Here, we set the spherical inner and outer boundaries at r = 0.1 and 1.5 ly. The primary boundary conditions for the RSG wind are given as density $\rho = 3000 \times m_p$ g/cm^3 (where m_p is proton mass), temperature $T = 5 \times 10^3$ K, radial velocity V_r = 10 km/s, and toroidal magnetic field $B_\Phi = B_0 \cos\theta$ with B_0 = 37 nT (where θ indicates the latitude). In addition, the polarity change is given for B_Φ across the equatorial plane with a neutral sheet width of 3.0°. Inside the neutral sheet, density is increased to balance with the magnetic pressure. Assuming a coronal hole at latitudes higher than 55.7°, the primary boundary conditions are modified there to give high-speed hot plasma, increasing V_r by a factor of 4.0 and increasing T by a factor of

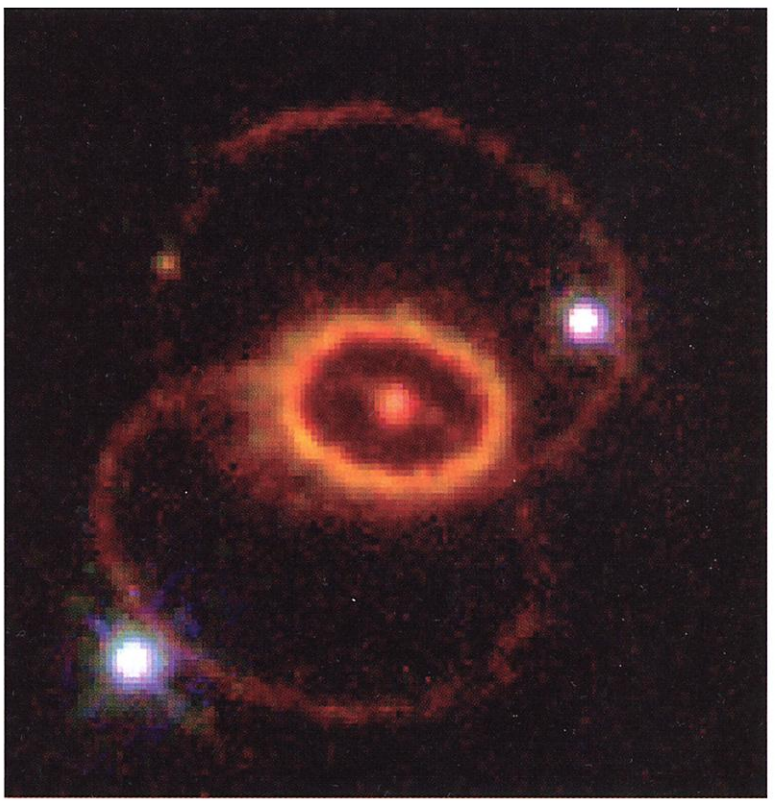

Fig. 1. The three-ring structure in the circumstellar space of the SN 1987A observed by the HST. The ER is on the equatorial plane, and the two ORs are near 45° latitudes. The original picture is rotated 90° for easy comparison with Fig. 2. (Space Telescope Science Institute image, also available at http://oposite.stsci.edu/pubinfo/jpeg/SN1987A_Rings.jpg)

[1]Communications Research Laboratory, Koganei-shi, Tokyo 184-8795, Japan. [2]Shonan Institute of Technology, Tsujido, Fujisawa 251-8511, Japan.

*To whom correspondence should be addressed. E-mail: tanaka@crl.go.jp

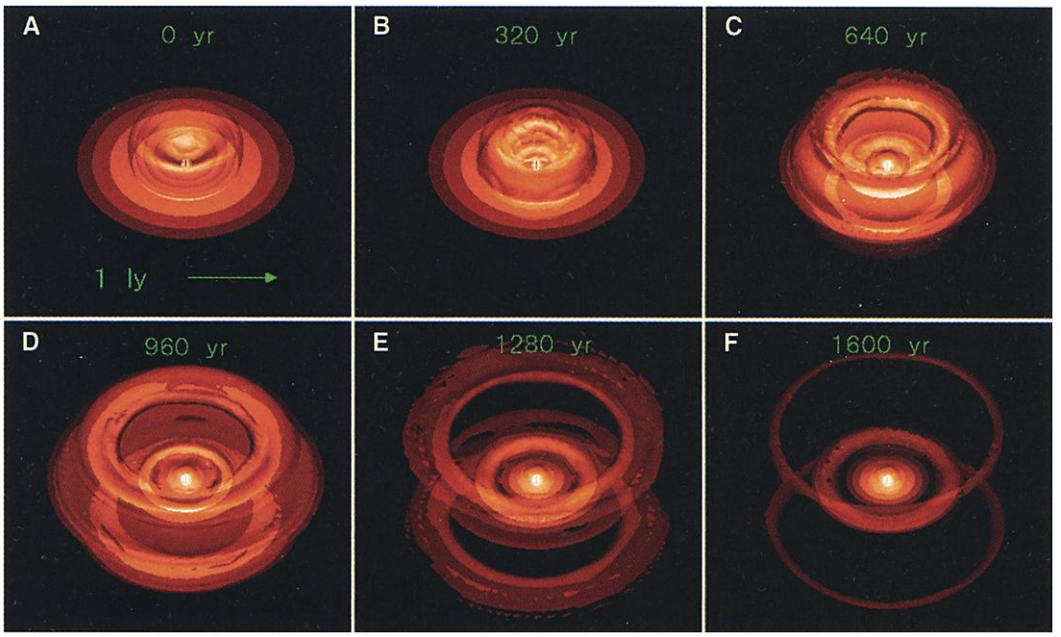

Fig. 2. Time sequence of simulated plasma density distribution around SN 1987A. Three-dimensional isodensity surfaces are shown at four number levels (0.12, 0.06, 0.04, and 0.03) × 3000 cm^{-3} for (**A**), an initial state when the star was a RSG, and (**B** to **F**), successive developments after the star had changed to a BSG. White spheres show the position of the central star, and elapsed times after the SN explosion are indicated.

2.0. Despite this modification, the fluxes ρV_r and $B_\Phi V_r$ are held unchanged at all latitudes. Similarly, the primary boundary conditions for the BSG are specified as $\rho = 55 \times m_p$ g/cm^3, $T = 4 \times 10^4$ K, and $V_r = 460$ km/s. In the coronal hole region of BSG at latitudes higher than 21.1°, V_r is increased by a factor of 3.0; at latitudes lower than 21.1°, V_r is reduced by a factor of 0.5, under the assumption that the flow is decelerated before reaching the inner boundary because of the relative density of the plasma. Among these boundary conditions, latitudes of the coronal hole are determined by iterating the MHD model. Other primary boundary conditions are taken from the literature [(*3*) and references therein].

The three-dimensional structure of the steady RSG wind, obtained after a sufficient time of numerical integration under a fixed set of RSG inner boundary conditions, shows that the density essentially falls with r as r^{-2} because of the radial expansion (Fig. 2A). The disk-like structure shows dense neutral sheet plasma in the equatorial plane. This density enhancement is due to the equatorward magnetic-pressure force (pinch effect) of B_Φ. The density is relatively low in the high-latitude coronal hole where the wind speed is high. In addition, broad density enhancement occurs on the low-latitude sides of the boundary at 55.7°. This density increase, although not as visible as the equatorial disk, is due to the poleward compression of plasma by the magnetic pressure.

The evolution of the density distribution in the circumstellar space after the BSG wind is turned on at the inner boundary indicates that the BSG wind is almost invisible because its density is low. Therefore, the evolution of the density distribution shown here is generated by the redistribution of RSG plasma in the course of the wind-wind interaction. The high-speed flow induced by the BSG wind sweeps up the RSG plasma in the circumstellar space in front of the contact surface. Then this surface of dense RSG plasma is inflated like a balloon (Fig. 2, C and D). At this stage, RSG plasma in the polar region is blown off by the fast BSG flow. In the course of the inflation, local concentrations of RSG plasma occur in three latitudinal regions: one at the equator corresponding to the ER, and two at the northern and southern mid-latitudes corresponding to the ORs. Near the equator, B_Φ originally distributed in the RSG wind and swept up in front of the contact surface exerts a magnetic pinch effect to accelerate the ER formation.

In the ORs, the magnetic intensity and plasma density become greater than those of the surrounding region because both components are compressed simultaneously under the frozen-in condition. Hence, the ORs are confined not by the surrounding magnetic pressure but by the thermal pressure built up by the fast BSG wind so as to surround the ORs. The BSG wind is decelerated more severely around high-density ring areas (Fig. 2C). This deceleration in turn generates high-pressure walls around the ORs and spurs the ring formation. Finally, the fast wind blows off RSG plasma in the crevices of the rings and makes the three rings stand out more (Fig. 2, E and F). At the final stage (Fig. 2F), the ratio of the OR radius to the ER radius is 2, which is just the same as the HST observations (*6*), and the density ratio of the ER to the OR is about 3, which coincides well with the observational value of 2 to 4 (*7*). The density contrast between the ORs and the surrounding plasma is 30 on the front side and 3 on the back side. The radial velocity of the ORs is 57.5 km/s, which is faster than the observed value of 26 km/s (*8*).

The final shape of the ring structure depends on the parameters of the RSG and BSG; hence, it may be possible to study the configuration of stars in the final stage of their lives by finding simulation parameters that generate the rings actually observed. Our simulation suggests that the structures of the RSG and BSG exhibit many similarities to those of the Sun. The formation process of the ORs indicates that both the RSG and BSG should have magnetic fields resembling that of the Sun. The intensity of the magnetic pressure in the RSG wind should be of the same order of magnitude as that of the thermal pressure. Moreover, the RSG and BSG should also have high-speed polar streams resembling that of the Sun. To obtain a steady state of RSG wind, it is necessary to integrate the MHD equation under a steady condition for 36,000 years. Our results suggest an RSG wind that has been blowing fairly steadily for a long period before the BSG phase, in contrast to the solar wind, which is always undergoing long- and short-period variations.

References and Notes

1. S. Kwok, *Astrophys. J.* **258**, 280 (1982).
2. J. M. Blondin, P. Lundqvist, *Astrophys. J.* **405**, 337 (1993).
3. H. Washimi, S. Shibata, M. Mori, *Publ. Astron. Soc. Jpn.* **48**, 23 (1996).
4. J. L. Phillips *et al.*, *Geophys. Res. Lett.* **22**, 3301 (1995).
5. T. Tanaka, *J. Comput. Phys.* **111**, 381 (1994).
6. C. J. Burrows *et al.*, *Astrophys. J.* **452**, 680 (1995).
7. S. P. Maran *et al.*, *Astrophys. J.* **545**, 390 (2000).
8. A. P. S. Crotts, S. R. Heathcote, *Astrophys. J.* **528**, 426 (2000).
9. We thank S. Shibata for discussions.

28 December 2001; accepted 8 March 2002